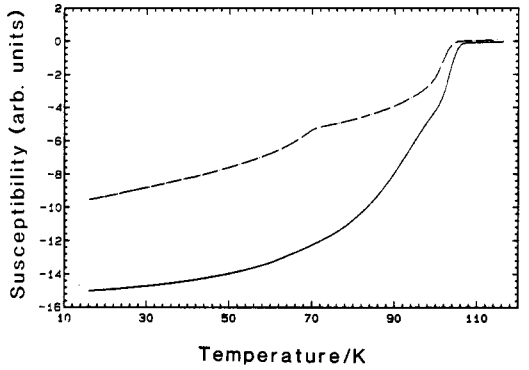

Figure 11. Ac susceptibility measurements of materials precipitated at pH 7 (dashed) and 8 (solid), following heating at 860 and 870 °C.

peaks characteristic of $Bi_{1-x}Pb_xCaSr_2Cu_2O_8$ (-2122) and show little pH dependence (Figure 9). Other peaks are mostly attributable to Ca_2PbO_4.

After the heatings at 860 °C, all samples showed roughly equal amounts of the -2122 and -2223 phases. However, following the 870 °C treatment, clear differences and trends are to be seen in the XRD patterns (Figure 10). The pH 7 sample shows a mixture of comparable amounts of the -2122 and -2223 phases. Since we saw (Figure 1, bottom) a substantial loss of Ca at this pH, this is not surprising, since there is a greater requirement for Ca (sandwiched between the CuO sheets) in the -2223 form. The pH 8 pattern shows nearly single-phase -2223, and this is confirmed in ac susceptibility measurements (Figure 11), where only a slight deviation from the single transition at 107 K is to be seen. This is in marked contrast to the clear double transition observed for the pH 7 sample. The XRD pattern for pH 9 is very similar to that of pH 8. As the pH is increased further, however, the concentration of the -2122 phase steadily increases (Figure 10). This may be due to the increased lead loss above pH 9 (Figure 1, top), since lead is a well-known promoter of the -2122 to -2223 reaction.[9,10]

Summary and Conclusions

TMA_2CO_3/TMAOH precipitation of precursors to the Bi-Pb-Ca-Sr-Cu-O system is an efficient method of placing the metal ions in intimate contact with each other prior to calcination. Precise stoichiometric control can be maintained, provided that the pH is held at around 8 or 12 during the entire precipitation. pH 8 is preferable, since pH 12 leads to larger crystallites, which reduce homogeneity, and smaller agglomerates, which extend filtering times.

With the exception of the material formed at pH 6, which was extremely deficient in Ca and Sr and melted at <800 °C, all precipitates ultimately formed a mixture of the -2122 and -2223 structures when calcined first at 800 °C and then at 860 and 870 °C. The sample initially precipitated at pH 8 seems to produce the most phase-pure -2223 material.

Acknowledgment. I am very grateful to Ted Peders for his skillful sample preparation and to Jane Swain, Bob Collins, and Eric Taylor for their analytical assistance.

Registry No. $Bi_{1.8}Pb_{0.2}Sr_2Ca_2Cu_3O_{10}$, 118903-34-7; tetramethylammonium carbonate, 40105-52-0.

(9) Takano, M.; Takada, J.; Oda, K.; Kitaguchi, H.; Miura, Y.; Ikeda, Y.; Tomii, Y.; Mazaki, H. *Jpn. J. Appl. Phys.* **1988**, *27*, L1041-L1043.
(10) Green, S. M.; Jiang, C.; Mei, Y.; Luo, H. L.; Politis, C. *Phys. Rev. B* **1988**, *38*, 5016-5018.

Growth of Zeolite Crystallites and Coatings on Metal Surfaces

Shawn P. Davis,[†,‡] Eric V. R. Borgstedt,[‡] and Steven L. Suib*[,†,‡,§]

Department of Chemistry, Institute of Materials Science, and Department of Chemical Engineering, U-60, University of Connecticut, Storrs, Connecticut 06269-3060

Received May 11, 1990

Zeolite crystals have been grown on metal surfaces by modified hydrothermal alteration methods. Coatings of zeolites can be grown in thicknesses ranging from 1 μm to about 1 mm. Zeolite crystals can be selectively bonded to one side of the metal substrate due to gravitational effects during the zeolite crystallization. Several types of syntheses have been successful, such as the growth of crystals at metal surfaces directly in the autoclave and growth of zeolites at metal surfaces that have been spin coated or immersed in various mother liquors. The zeolites have been characterized by X-ray powder diffraction, scanning electron microscopy, luminescence spectroscopy, 180° peel strength measurements, and surface area measurements. Details of the synthetic preparation are also discussed. The purpose of making such coatings is to prepare new materials with possible uses in such areas as electrochemistry, catalysis, adsorption, sensor applications, semiconductor circuitry, and photochemistry.

I. Introduction

Thin films are typically composed of metals or semiconductors.[1] Preparative methods of thin films include vapor deposition, radio frequency sputtering, and laser beam deposition.[2] The thickness of films can be monitored in a variety of ways including piezoelectric quartz crystals, X-ray fluorescence, eddy current measurements,

Table I. Scotch Tape 180° Peel Strength Measurements (51 mm/min) of Various Thicknesses of Zeolite Coatings on Copper Foil (Values in g/mm)

sample	first trial	second trial
thick zeolite coating (1 mm)	1	24
intermediate zeolite coating (<0.5 mm)	18	47
thin zeolite coating (<0.5 mm), Eu^{3+} exchanged	32	38

[†] Department of Chemistry.
[‡] Institute of Materials Science.
[§] Department of Chemical Engineering.
* To whom correspondence should be addressed at the Department of Chemistry.

0897-4756/90/2802-0712$02.50/0

and β backscattering. Typical thicknesses range from 50 to 500 Å. The lateral and depth uniformities of thin films often control their chemical and physical properties.

Thin films have several applications as catalysts, electrode sensors, coatings for optical devices, adhesives, and corrosion-resistant films.[3] Often the structural and chemical properties of the thin films are not exactly the same as those of bulk solids. For electrical devices it is important to know whether or not pinholes are present between the surface of the thin film and the substrate onto which the film has been deposited. Pinholes can lead to electrical shorts and eventually to breakdown of the film.[4]

There is a need for thin films and coatings of materials that can be synthetically altered after deposition of the thin film. Semiconducting films can indeed be doped after being deposited as thin films, but the resulting films may not be uniformly doped or as rugged as materials deposited within chemical or physical treatments.[5] In the fields of ceramics and catalysis, rugged thin films capable of withstanding high temperatures are needed. Such materials are usually insulators and cannot be deposited with traditional thin-film synthetic procedures.[6]

Zeolites are a class of insulating materials that are porous molecular sieves. Zeolites are aluminosilicates that have exchangeable cations. Therefore, the chemical compositions of zeolites can be controlled over a wide range. Zeolites are also quite thermally stable. Temperatures above 500 °C are typically used in cracking reactions of hydrocarbons in zeolite catalysts.[7a]

There are clearly several attractive features of zeolites that would make then useful in designing molecular thin-film and coated materials that could be utilized for a variety of purposes. Researchers at W. R. Grace, Davison Division, prepared coatings of zeolites on glass by hydrothermal alteration processes.[7] Magnetic particles have also been coated with zeolites by researchers at Exxon in order to prepare magnetic fluidized beds.[8] Ozin et al.[9]

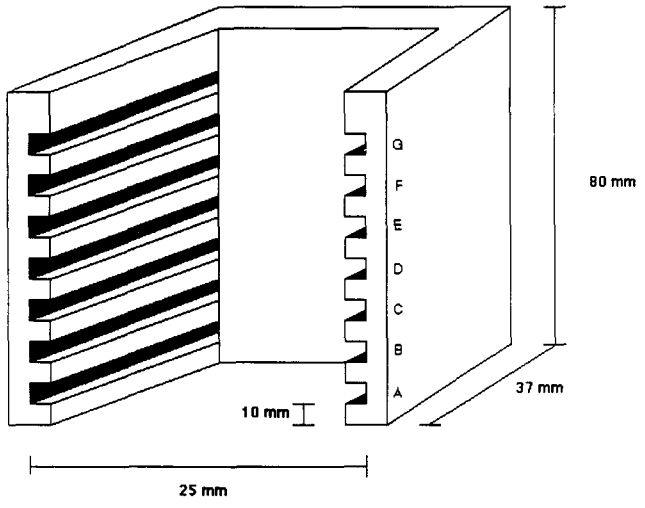

Figure 1. Diagram of apparatus used to prepare zeolite coatings of various thicknesses on copper foils.

have recently discussed applications of zeolites for sensors, quantum dots, electronics, batteries, membranes, and nonlinear optical materials.

Zeolites are three-dimensional extended structures as are most inorganic compounds. Organometallic compounds are an obvious exception to this structural classification. Since thin films and coatings are basically two-dimensional by nature, it would seem a difficult task to prepare thin films of zeolites especially by using standard thin-film preparation techniques. Nevertheless, permselective inorganic membranes described by Armor are attractive separators.[10] Zeolite membranes grown on glass, as well as some preliminary work with metals and metal oxides, have been studied by Suzuki.[11] Coatings of zeolites that have been studied so far include polymer hosts. In these systems, zeolites particles have been dispersed in polymers followed by coating and cross-linking. Applications in the areas of gas adsorption[12] and electrochemical sensors[13] have been made.

For several years we have been attempting to make thin films of zeolites on metal substrates. Resistive heating,[14] electrochemical syntheses,[14] tin oxide coatings,[15] radio frequency sputtering, and other more traditional methods of thin-film deposition have failed to produce thin crystalline films of zeolites on any substrate.

We report here that crystals of zeolites can be prepared on metal surfaces by modified hydrothermal alteration procedures. Although copper was used for the majority of experiments, zeolite coatings were also formed on silver, platinum, titanium, molybdenum, iron, and tin. Details of the synthetic procedures and their implications for the deposition of zeolites on metal surfaces will be discussed. These zeolite materials have been characterized with X-ray powder diffraction methods (XRD), scanning electron microscopy (SEM), luminescence spectroscopy, 180° peel

(1) Klabunde, K. J. *Thin Films from Free Atoms and Particles*; Academic Press: New York, 1985.

(2) (a) Berry, R. W.; Hall, P. M.; Harris, M. T. *Thin Film Technology*; Van Nostrand: Newark, New Jersey, 1968. (b) Ferrieu, F.; Vu, D. P.; D'Anterroches, C.; Oberlin, J. C.; Maillet, S.; Grob, J. J. *J. Appl. Phys.* **1987**, *62*, 3458–3461. (c) Biegen, J. F.; Smythe, R. A. SPIE O/E LASE Symposium, 1988, Los Angeles, CA. (d) Weissman, J. G.; Burke, P. A.; Ko, E. I.; Wynblatt, P. *J. Chem. Soc., Chem. Commun.* **1989**, 329–330. (e) Niwa, M.; Hibino, T.; Murata, H.; Katada, N.; Murakami, Y. *J. Chem. Soc., Chem. Commun.* **1989**, 289–290. (f) Pickett, C. J.; Ryder, K. S. *J. Chem. Soc., Chem. Commun.* **1988**, 1362–1364. (g) Roberston, J. L.; Moss, S. C.; Liftshitz, Y.; Kasi, S. R.; Rabalais, J. W.; Lembert, G. D.; Rapaport, E. *Science* **1989**, *243*, 1047–1050. (h) Bent, B. E.; Nuzzo, R. G.; Dubois, L. H. *J. Am. Chem. Soc.* **1989**, *111*, 1634–1644. (i) Bachmann, P. K.; Messier, R. *Chem. Eng. News* **1989**, *67*, May 15, 24–29. (j) Jensen, J. A.; Gozum, J. E.; Pollina, D. M.; Girolami, G. S. *J. Am. Chem. Soc.* **1988**, *110*, 1643–1644. (k) Dong, S.; Sun, Z.; Lu, Z. *J. Chem. Soc., Chem. Commun.* **1988**, 993–995.

(3) Good, M. L. *Biochemistry and Materials Science*; American Chemical Society: Washington, DC, 1988.

(4) Bard, A. J.; Faulkner, L. R. *Electrochemical Methods*; Wiley: New York, 1980.

(5) (a) Tachibana, H.; Nakamura, T.; Matsumoto, M.; Komizu, H.; Manda, E.; Niino, H.; Yabe, A.; Kawabata, Y. *J. Am. Chem. Soc.* **1989**, *111*, 3080–3081. (b) Wu, X. L.; Lieber, C. M. *J. Am. Chem. Soc.* **1988**, *110*, 5200–5201.

(6) (a) Kawamura, S.; Tsutsui, T.; Saito, S.; Murao, Y.; Kina, K. *J. Am. Chem. Soc.* **1988**, *110*, 509–511. (b) Luk, S. Y.; Williams, J. O. *J. Chem. Soc., Chem. Commun.* **1989**, 158–159. (c) Bain, C. D.; Troughton, E. B.; Tao, Y. T.; Evall, J.; Whitesides, G. M.; Nuzzo, R. G. *J. Am. Chem. Soc.* **1989**, *111*, 321–335.

(7) (a) *Fluid Catalytic Cracking*; Occelli, M. L., Ed.; ACS Symposium Series, No. 375: American Chemical Society: Washington, DC, 1988. (b) Albers, E. W.; Edwards, G. C. U.S. Patent 3,730,910, 1973.

(8) Hoving, K.; Walterbos, J. W. M. U.S. Patent 4,578,372, 1986.

(9) Ozin, G. A.; Kuperman, A.; Stein, A. *Angew. Chem., Int. Ed. Engl.* **1989**, *28*, 359–376.

(10) Armor, J. N. *Appl. Catal.* **1989**, *49*, 1–25.

(11) (a) Suzuki, H.; Abstracts 3rd Chem. Congr. of N. America, 1988, Toronto, Petroleum Division; p 73. (b) Suzuki, H. U.S. Patent 4,699,892, 1987.

(12) (a) Bein, T.; Carver, R. F.; Farlee, R. D.; Stucky, G. D. *J. Am. Chem. Soc.* **1988**, *110*, 4546. (b) Bein, T.; Brown, K.; Frye, G. C.; Brinker, C. J. *J. Am. Chem. Soc.* **1989**, *111* 7640–7641.

(13) (a) *Chem. Eng. News* **1988**, *66*, July 4, 29. (b) Shaw, B. R. In *Electrochemistry, Past and Present*; ACS Symposium Series, No. 390; American Chemical Society: Washington, DC, 1989; pp 318–338. (c) Shaw, B. R.; Creasy, K. E. *J. Electroanal. Chem.* **1988**, *234*, 209–217.

(14) Faulkner, L. R.; Suib, S. L.; unpublished results.

(15) Coughlin, D. F., Ph.D. thesis, University of Connecticut, 1985.

strength measurements, and surface area measurements.

II. Experimental Methods

A. Synthesis of Zeolites. All metal foils were initially etched to enhance adhesion as described in section II.A.1. Five different preparations of zeolite crystallites and coatings are described in sections II.A.2–5.

(1) Etching of Metal Surfaces. Copper metal foils were treated with 2.2 M KOH in ethanol solutions for 1 h with stirring at room temperature. This was followed by a rinsing with distilled water. Concentrated HCl was then placed over the metal surface and stirred for 0.5 h at room temperature. The metal foil was then rinsed with distilled water followed by washing with 18 MΩ distilled deionized water (DDW).

Some metal foils were further treated in an additional step by washing for 0.5 h with an aqueous 1 M NaOH solution followed by rinsing with distilled water and then with DDW. This last step was done to remove surface Cl^- introduced during the second surface treatment step described above.

(2) Substrate Leaning on Autoclave Wall. Initial attempts were made to grow zeolites on copper metal surfaces by leaning a piece of copper metal foil having dimensions 19 mm × 13 mm × $^1/_2$ mm on the wall of a Teflon-lined Morey autoclave reactor. The composition of the gel precursor was $11Na_2O{\cdot}Al_2O_3{\cdot}27SiO_2{\cdot}366H_2O$, and the raw materials were Ludox AS-40 from Du Pont, NaOH from Alfa Ventron, Danvers, MA, and Catapal alumina from Conoco, Inc. Synthesis conditions were similar to those described in steps 1–5 in section II.2.4. Samples were heated at 96 °C under autogeneous pressure for various times such as 11, 24, 35, and 48 h. After nucleation the copper foil was removed from the autoclave, washed with DDW, and dried in air at room temperature for 24 h.

(3) Substrates Horizontal and Elevated in Autoclave. Several copper foils were mounted horizontally at 10-mm spacings in a Teflon holder in a Teflon-lined Parr autoclave. Conditions used for this synthesis were as described in section II.A.2.4 although only steps 1–5 were followed. For example, the mother liquor was not separated and filtered out from the bulk. A diagram of the Teflon holder used in this procedure is given in Figure 1. The Teflon holder, containing several pieces of copper metal foil, was placed at the bottom of the Teflon-lined autoclave before the gel is added. Conditions for crystallization, washing, and drying were similar to those described in section II.A.2. The pieces of metal foil were placed, while still in the Teflon holder, in DDW after the synthesis and the DDW was replaced three times in 1 h followed by drying of the samples in air at room temperature for 24 h.

(4) Synthesis of Mother Liquor. Nine steps are used in the preparation of the mother liquor. Step 1 is the preparation of sodium aluminate. In a stainless steel reactor 217.10 g of DDW and 48.90 g of NaOH are dissolved and heated to 80 °C. At 80 °C, 8.00 g of Al_2O_3 is added while stirring. This is heated to 110 °C until all of the Al_2O_3 dissolves and then continuing for 5 min longer. This solution is then cooled to room temperature.

Step 2 involves weighing 225.45 g of Ludox AS-40 in a Nalgene beaker. Step 3 comprises the addition of the sodium aluminate solution to the Ludox and stirring the gel until it is homogeneous. Step 4 entails pouring the homogeneous gel into a Teflon-lined Parr autoclave (liner capacity is 900 mL), covering with a Teflon cap, and sealing the autoclave. The mixture in the autoclave is allowed to stand for 24 h at room temperature for initial nucleation in step 5.

Step 6 involves placing the autoclave in an oven set at 96 °C for 6 h. In step 7 the autoclave is removed from the oven and quenched in a static water bath for 1.5 h. To obtain a maximum amount of mother liquor, the resulting sol–gel mixture is poured through a Buchner funnel in step 8, and the mother liquor is filtered several times to ensure exclusion of macroscopic particles. The liquor is then used for preparation of coatings on metals, and the solid bulk material is washed with DDW and dried in an oven at 80 °C in step 9. The zeolite coatings on metals are retained for X-ray powder diffraction and other experiments.

(5) Mother Liquor Spin Coated onto Substrate. An aged gel prepared as described in section II.A.4 was used for spin-coating studies. After initial reaction a mother liquor formed on top of the gel. In this case the slides were cleaned as mentioned in section II.A.1 (no NaOH wash), but they were then dried in a vacuum dessicator. About 1 mL of the liquor, added dropwise, was deposited onto a copper foil spinning at greater than 180 rpm. This material was allowed to spin for several minutes and then put into a Parr autoclave and heated at 96 °C under autogeneous pressure for 24 h.

(6) Substrate Immersed in Mother Liquor. Mother liquor such as that described in section II.A.4 was used to prepare zeolites on metal foil by placing the foil at the bottom of a Parr autoclave, pouring the mother liquor over the foil, and heating this material to 96 °C for 12 h. The resultant material was washed, filtered, and dried at room temperature.

B. Characterization Methods. (1) X-ray Powder Diffraction. A Philips X-ray powder diffractometer was used to determine the crystalline phases present after nucleation on the copper surfaces. For these experiments copper foils of 20 mm × 20 mm × $^1/_2$ mm were used so that these samples could be directly inserted into the sample holder on the diffractometer. A Ni filter and Cu Kα radiation were used to scan from 10° to 60° 2θ at 2°/min. The d spacings, intensities, and hkl values were compared to known values for several zeolites. Synchrotron X-ray diffraction (XRD) experiments were done at the University of Connecticut Health Center with a rotating anode X-ray source and a wire detector. Zeolite-coated metal slides were mounted perpendicular to the radiation source.

(2) Scanning Electron Microscopy. Scanning electron microscopy analysis of the zeolite crystals grown on the copper foils were done on an Amray SEM Model 1000 with a Model 9100 energy dispersive X-ray (EDX) analyzer, on an AMRAY Model 1200 SEM and on an AMRAY/LICO Model 1810 D SEM equipped with a Model 9800 energy dispersive X-ray analyzer. Samples were quite conductive, and there was no need to coat these samples.

(3) Luminescence Excitation and Emission. Luminescence spectra were recorded on a Spex Model 1680 luminescence spectrometer. Samples of 25 mm × 8 mm × $^1/_2$ mm were used for these experiments, and these materials were inserted into UV-grade quartz cuvettes. Front-face mode excitation and emission experiments were performed.

(4) Surface Area and Pore-Size Measurements. Surface area and pore-size distribution measurements were done with a Omicron Model Omnisorp 100CX analyzer. Samples were dehydrated in a vacuum before Ar adsorption. The samples were heated at a rate of 25 °C/0.5 h from room temperature to 125 °C. The samples were held at 125 °C for 2 h. After 2 h the temperature was increased at 50 °C/h until the temperature of 375 °C was reached. The samples were held at 375 °C for 12 h. A plot of $P/V_{ads}(P_0 - P)$ vs P/P_0 was made to determine surface areas. A plot of the derivative of V/P vs effective pore diameter was made to determine the pore size distribution.

C. Modification of Thin Films. (1) Ion Exchange. An elevated Teflon platform above a magnetic stir bar was placed in a 500-mL beaker for ion-exchange experiments. Samples of zeolites grown on copper metal foils were placed on this platform, and the platform was immersed in 300 mL of a 0.001 M solution of $Eu(NO_3)_3{\cdot}5H_2O$ and stirred for 24 h. These samples were then washed with 500 mL of DDW, filtered, and dried in air for about 24 h.

(2) Mechanical Stability. Samples of zeolites grown on copper foil were studied for 180° peel strength with an Instron Model 1011 apparatus to determine the relative strength of bonding of the zeolite to the metal surface. In addition, samples were placed in a Bransonic ultrasonic cleaner (tank capacity = 2.8 L, cleaning power = 100 W) for 24 h and were subsequently analyzed with an AMRAY/LICO Model 1810 D SEM equipped with an energy dispersive X-ray analyzer.

III. Results

A. Synthesis. Copper metal foil substrates, when leaned against the side of an autoclave during zeolite synthesis, obtain a solid coating of zeolite. The zeolite coating uniformly increases in thickness as the depth of immersion increases. A black coating of copper oxide is formed on the surface of copper metal when the copper is out of the sol.

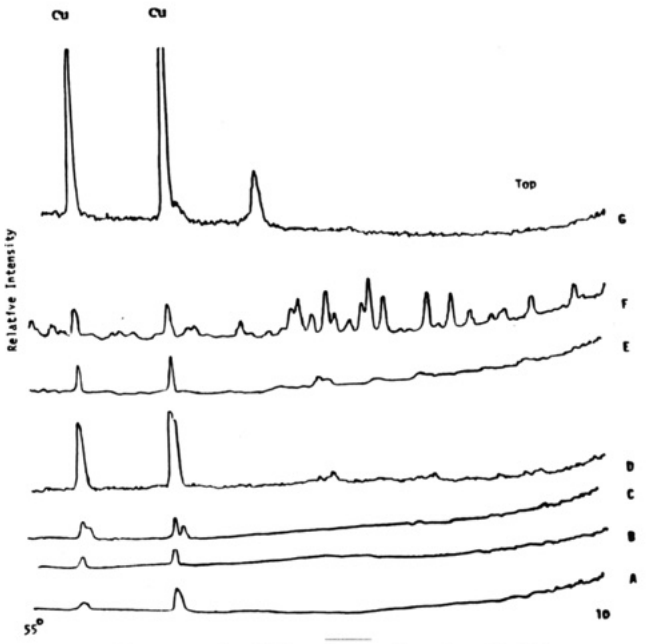

Figure 2. X-ray powder diffraction studies of zeolite Y on copper foils grown at different levels in autoclave: (A) = 1 cm from bottom; (B) 1 cm above A, etc.

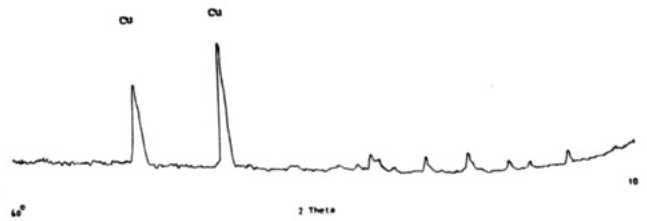

Figure 3. X-ray powder diffraction data for zeolite Y grown by the immersion method.

No growth of zeolite is observed on the bottom side of the copper foil after the zeolite copper materials are removed from the autoclave. No such growth was observed in any of the experiments.

A Teflon holder with slots at various heights as shown in Figure 1 was used to hold metal foils horizontally in the autoclave during synthesis. In this configuration zeolite crystals grew only on the top side of the metal surface. In addition, thinner coatings formed at positions higher up in the autoclave as long as the copper foil was immersed in the gel or mother liquor.

When zeolite syntheses were interrupted after short periods of time (about 6 h) before extended crystallization, it was noted that the top part of the gel precursor was like a sol and the bottom part was more viscous, like a gel. The thinnest coatings of zeolite were found to grow in the upper sol part of this mixture.

X-ray powder diffraction patterns of zeolite Y crystals deposited at the various levels of the Teflon autoclave after 12 h are shown in Figure 2. The XRD pattern of bulk zeolite Y prepared in the absence of metal substrate from the same preparation is crystalline and matches that of Na–Y zeolite. In lower parts of the autoclave, after a synthesis time of 24 h, thick coatings of zeolite Y were obtained. At long times (≥12 h) extra diffraction lines for zeolite P were also observed for samples that were grown in the upper regions of the sol.

Small amounts (<200 mL) of the sol were removed from the autoclave after 6 h of reaction and were used to spin coat metal substrates that were then put back into an empty autoclave. The surface of the copper foil oxidized significantly for these spin-coated samples, producing a green coating on the surface. In addition, excess sol was used to cover metal substrates placed at the bottom of the autoclave. An X-ray powder diffraction pattern of a thin coating of zeolite Y on copper grown by this immersion method is shown in Figure 3 for comparison. X-ray diffraction patterns similar to that of Figure 3 were obtained for all of the materials prepared by the various methods

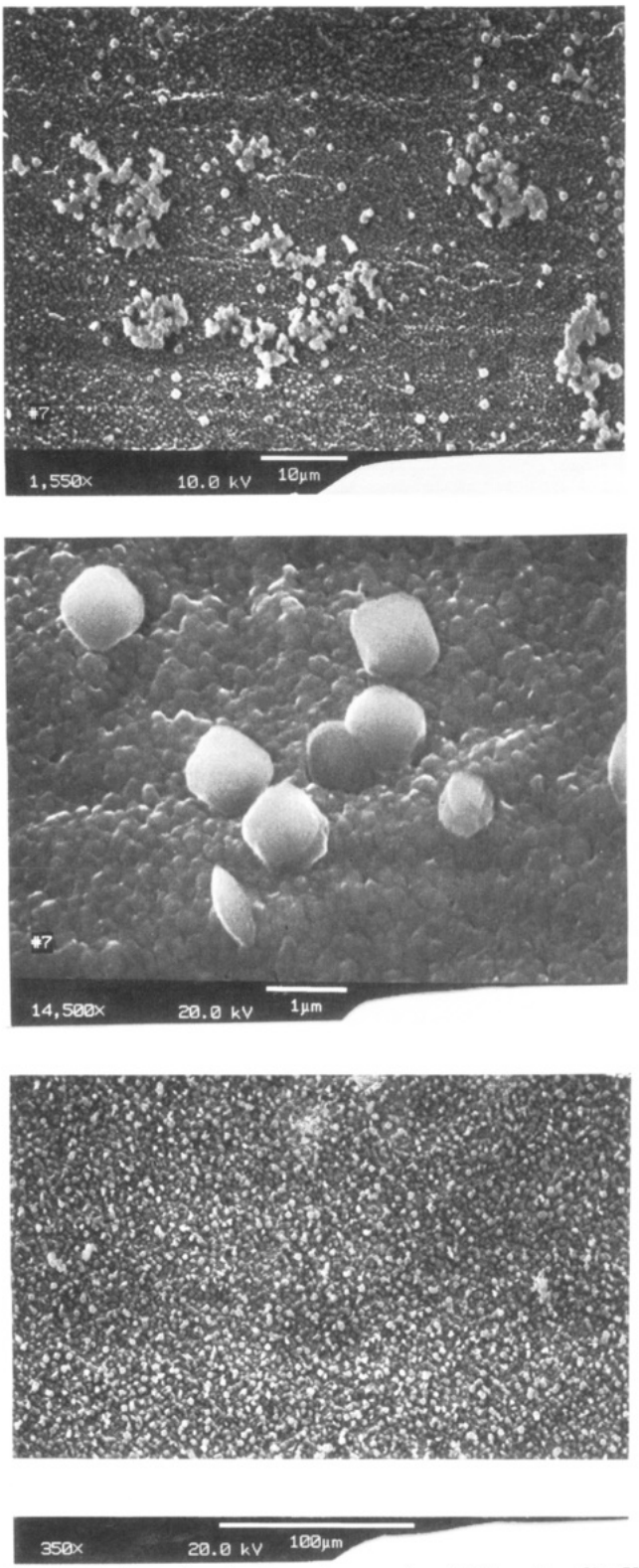

Figure 4. Scanning electron micrographs of different zeolite Y thicknesses on copper foil: (top) thin coating; (middle) isolated crystals; (bottom) thick coating.

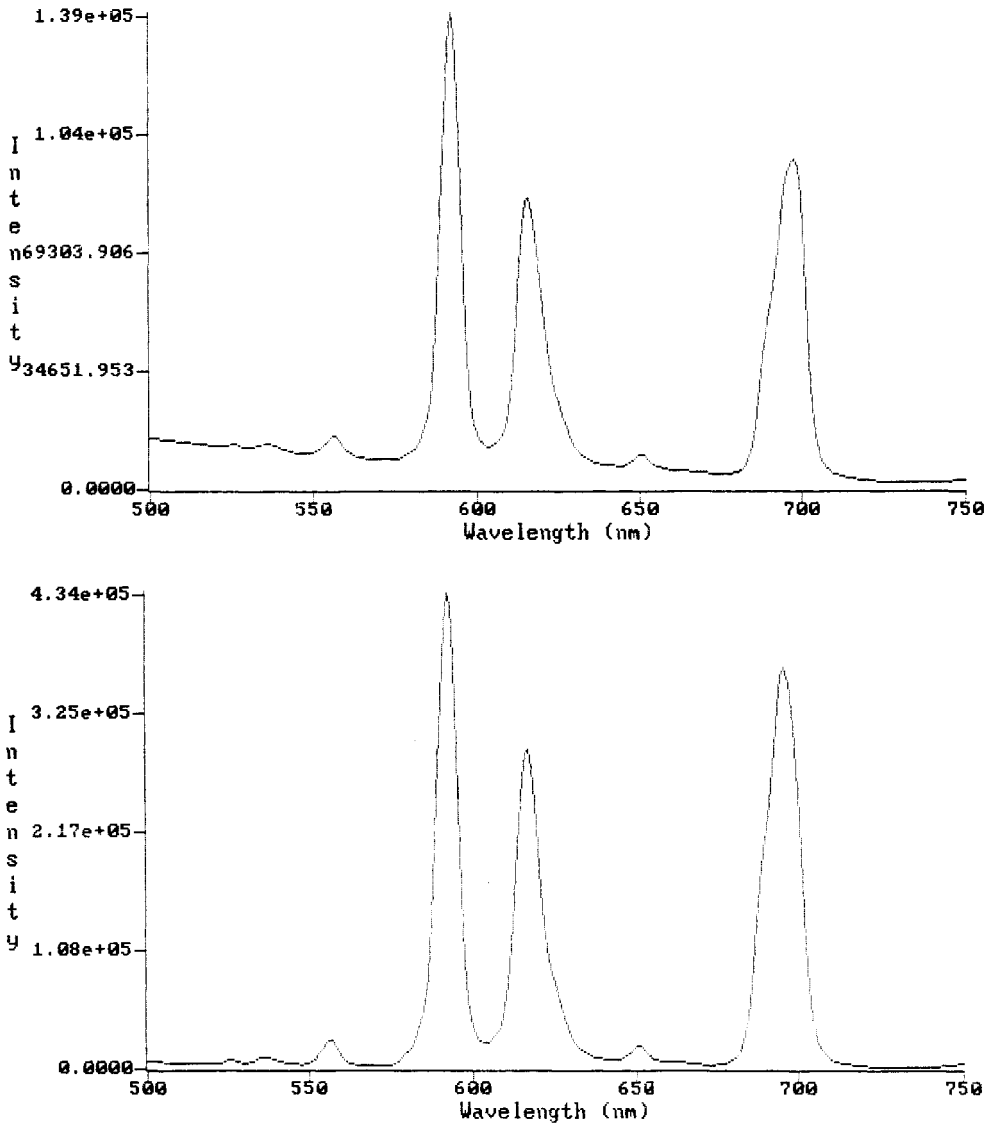

Figure 5. Luminescence emission spectrum of Eu^{3+} ions exchanged into (top) zeolite Y grown on copper foil and (bottom) bulk zeolite Na–Y.

described in this section. Scanning electron micrographs of copper foil immersed in mother liquor and reacted for various amounts of time are shown in Figure 4. Zeolite coatings formed by the immersion method were more uniform than materials grown by the spin-coating method. For the most thinly coated samples having isolated crystals embedded in the metal surface, no diffraction pattern was observed by routine XRD experiments. These materials are crystalline as evidenced by synchrotron XRD experiments that show diffraction of the major d spacings of Na–Y zeolite. In general, shorter reaction times for all these types of preparations lead to more highly dispersed zeolite crystals and thinner coatings.

B. Ion-Exchange Properties. Zeolite Y thin coatings prepared by immersion methods were ion exchanged with $Eu(NO_3)_3 \cdot 5H_2O$ as described above. The luminescence emission spectrum of the dried Eu(III)-exchanged Y zeolite is given in Figure 5, top. For comparison the luminescence spectrum of Eu(III)-exchanged Y zeolite exchanged into the bulk powdered form is given in Figure 5, bottom. These luminescence bands are assigned to the Eu^{3+} ion. Such experiments were done on even the most dispersed systems, and similar luminescence spectra were observed. No loss of crystallinity or mechanical strength was observed after ion exchange.

C. Microanalysis. A typical energy dispersive X-ray (EDX) analysis of the immersed zeolite crystals deposited on etched copper is shown in Figure 6A. EDX analyses showed the presence of Na, Si, Al, O, Cl, and Cu. An EDX analysis for the same material except for an area between the zeolite crystals is given in Figure 6B.

D. Surface-Area and Pore-Size Measurements. Surface-area measurements of zeolite Y formed from the gel precursor given above and the bulk zeolite Y formed during the synthesis of zeolite coatings on metal foils lead to values of about 919 m^2/g. The effective pore size diameter for these samples as well as thick, medium, and thin zeolite coatings on copper foil is 0.7 nm.

E. Mechanical Stability. The 180° peel strength of several samples of various thicknesses is shown in Table I. The values for several standards are given in Table II.[16] After all of the zeolite-coated copper foil samples were analyzed, zeolite was still observed on the foils so the 180° peel strength measurements were repeated at the same place, and both values are shown in Table I. After exposure of a slide with a thick zeolite coating to ultrasonic cavitation for 24 h, it was analyzed by SEM. A photograph

(16) *Handbook of Adhesives*; Skeist, I., Ed.; Van Nostrand Reinhold: New York, 1977; pp 588–589.

Table II. Versalon 1138[a]/Additive and 90/10 Melt Blends 180° Peel Strength Measurements (51 mm/min, Values in g/mm)

versalon 1138b/ additive type	bonderized steel (rigid) to flexible			
	plasticized vinyl	Mylar	canvas	untreated polyethylene
control, none	5336	57	191	13
amorphous polypropylene (Oletac 100, Aivsum)	277	247	454	9
piperylene-based resin (Wingtack 95, Goodyear)	206	95	152	76
N-ethyl-*o*,*p*-toluenesulfonamide (Santicizer B, Mosanto)	295	400	156	34
glycerol ester of hydrogenated rosin (Staybelite Ester 10, Hercules)	409	152	181	20
maleic-modified polyethylene (Epolene C-16, Eastman)	157	154	227	98
ethylene vinyl acetate copolymer (Elvax 260, Du Pont)	291	104	327	13
phenol–formaldehyde resin (Bakelite CKR 5254, Union Carbide)	277	45	266	21

[a] General Mills Chemicals, Inc. [b] Resin designed for specific adhesion to unplasticized ABS and plasticized vinyl.

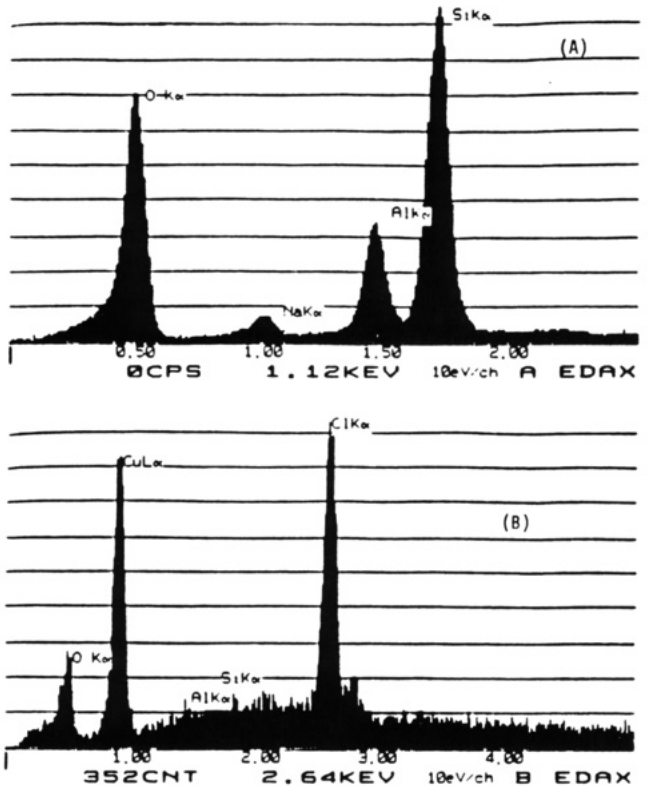

Figure 6. Energy dispersive X-ray analyses of zeolite Y grown on copper foil etched with HCl: (A) region on zeolite crystals; (B) region between zeolite crystals.

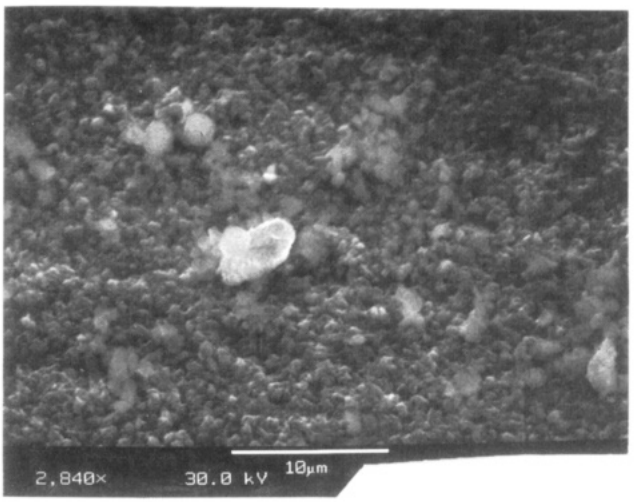

Figure 7. Zeolite Y on copper foil after 24 h of ultrasonic cavitation.

of this sample is shown in Figure 7.

IV. Discussion

A. Synthesis of Zeolite Y Thin Coatings. Initial experiments with copper foil leaned up against the wall of the autoclave showed that zeolites could grow on the copper foil as evidenced by X-ray powder diffraction experiments and that thicker coatings formed on the copper at lower depths of the gel. These experiments suggested that thin coatings might be produced by mounting copper foils horizontally further up in the gel and perhaps in the mother liquor phase, which separates out during aging and nucleation.

The holder shown in Figure 1 was designed to test these ideas. Results of various experiments with the metal substrates in different positions of the Teflon holder in the autoclave (Figure 1) suggest that secondary building blocks of the framework are forming above the metal substrate and then depositing on the metal. Gravity must play some role here since the zeolite crystals do not form on the bottom side of the metal substrate. Gravity effects in zeolites synthesis have been suggested by Thompson et al.[17] Since the thinner coatings grow in the upper sol portion of the sol–gel precursor, it seems that the aged and filtered mother liquor must contain zeolite precursor species that could be used for growth of zeolites.

Data of Figure 2 clearly show that crystalline zeolite Y is formed initially in the upper levels of the autoclave. Only further up in the sol phase are the more highly dispersed and isolated thinnest coatings formed. There is an ideal level for growth of these crystals since very high up in the sol relatively few crystals are formed.

The relative intensities of the diffraction peaks shown in Figure 2 for the zeolite crystal formed on the copper foil are similar to those of bulk zeolite Y.[18] Diffraction peaks for metallic copper are also observed in Figure 2 at 43.3° and 50.4° 2θ, which are expected for the copper metal substrates.

Results of spin-coating experiments and of experiments with excess sol covering metal substrates in autoclaves clearly show that the sol does contain suitable precursors

(17) Sand, L. B.; Sacco, A.; Thompson, R. W.; Dixon, A. G.; *Zeolites* **1987**, *7*, 387–392.
(18) Von Ballmoos, R. *Collection of Simulated XRD Powder Patterns for Zeolites*; Butterworths Scientific: Guilford, Surrey, UK, 1984.

for zeolite growth. These observations are consistent with the idea of a mother liquor as has been suggested in the literature.[19] It is quite probable that synthetic alterations of this mother liquor could lead to new and different phases of zeolites. Such will be the emphasis of another report.[20]

The preparation of other insulating thin-film coatings such as alumina, silica, metal oxides, nonmetal oxides, and other compositions that can be made into a gel should be possible with methods discussed here. In addition, other zeolites, clays, and pillared clay thin coatings might be prepared in this way.

Zeolite crystals prepared from the immersion technique yield well-defined crystals as shown in Figure 4 in SEM photographs. In fact, it is possible to grow such materials in restricted areas by preparing a mask and covering the areas that are not desired to be coated. Such coatings could be used in circuit board design.

B. Synthetic Modifications. The luminescence data of Figure 5, top, show that europium(III) ions can be exchanged into the zeolite Y thin coatings after synthesis of the coatings. The match of emission band intensities and positions between the zeolite Y thin coating and the europium(III) ion-exchanged bulk Y powder as shown in Figure 5, bottom, is quite good. We have previously shown[21] that the luminescence emission of solution and solid europium(III) coordination complexes, oxides, halides, hydroxide, and other types of ligands are all markedly different and can be used as a probe of the coordination environment of the Eu(III). It is even possible to distinguish the different Eu(III) environments of Eu(III)-exchanged X and Y zeolites, and the data of Figure 5a suggest that zeolite Y and not zeolite X is formed on the metal foils. This is surprising since the structure of X and Y are the same; the only difference is the Si/Al ratio and the concomitant cation content of these zeolites. In addition, luminescence emission spectra of Eu(III) P zeolites show luminescence emission different from that of both Eu(III) X and Y zeolites.

These luminescence data clearly show that the chemical composition of the zeolite Y thin coatings can be changed by synthetic means. No loss of zeolite was observed after ion exchange, although stirring during the ion exchange was done by protecting the coating from the Teflon-coated stir bar as mentioned in the Experimental Section.

Recent luminescence studies of Eu(III) X and Y zeolites have shown that hydrolysis of Eu(III) is more predominant in zeolite X than in zeolite Y.[22] Our data also suggest that Eu(III) ions in the zeolite crystallites and coatings are not hydrolyzed.

C. Thicknesses of the Zeolite Thin Coatings. The SEM data of Figure 4 suggest that the crystals growing on the copper foil are isolated with large uncoated areas of copper. Morphological studies of the Y zeolite crystals suggest from the rounded edge structure that the crystals are relatively flat, having a diameter of about 3 μm with thicknesses that are about 1 μm or smaller. This information can be deduced by tilting the samples in the SEM with concomitant observation of the crystal morphologies. For example, in Figure 4, top, there are some shapes that appear to be ellipsoidal. These crystals appear to be growing in cracks at the metal surface and suggest that the thickness of these crystals are on the order of tenths of microns. The conducting nature of the materials as observed by SEM, X-ray photoelectron spectroscopy,[23] scanning Auger microscopy,[23] and electrochemical experiments[24] also support this idea.

Scanning electron micrographs of the zeolite Y thick films such as those in Figure 4, bottom, do not show observation of the Cu substrate and indicate that laterally uniform zeolite thin films of interlinking crystallites have been produced. These materials may be of interest in applications where large amounts of zeolite are needed at the metal/foil interface. A particular example involves the use of zeolite/copper solar energy collectors such as those used in the Zeopower solar energy refrigerator cycle.[25] These materials rely on good heat transfer from the irradiated zeolite to the copper tubing. It is quite likely that direct bonding of the zeolite to the copper foil will allow better heat transfer than the nonbonded systems presently in use.

The surface area and pore size reported earlier clearly indicate that these materials are zeolitic in nature due to the typical adsorption isotherm data known to be found in zeolitic systems. Even thin coatings that could not be positively identified by XRD gave a pore size consistent with zeolite Y.

Microscopic studies have shown that the zeolite copper films do not charge as do insulating bulk powder samples. These observations suggest that zeolite crystallites are growing at the metal surface and are not merely nucleating in solution and depositing on the metal surface. In fact, zeolites deposited on surfaces from solution aggregate, develop a charge in surface and morphological experiments, and have different morphological and electrochemical[23] properties than materials reported here.

Thicknesses of these films are determined from cross sections in the SEM experiments for the thinnest coatings as well as from optical microscopy experiments on the thickest films.

D. Mechanical Stability. Although the thick coatings had small or negligible 180° peel strength values, which suggest that the zeolite/zeolite bond is weak, the values for thin coatings (<0.5 mm) and for thicker coatings (≥1.0 mm) analyzed at the same place for a second time were comparable to some of the polyamide adhesives shown in Table II. Polyamide adhesives are used in the shoe, automotive, and electronics industries.[16] Although the 180° peel strength values for the zeolite coatings on copper foil were probably enhanced by the Scotch tape adhesive, zeolite crystals were still observed on the surface of the foil after two measurements with the aid of an optical microscope (Nikon Optiphot 66, magnification 1000×). This suggests that the zeolite crystals are bonded to the foil and that the zeolite/metal interface is very strong. This is further supported by the fact that zeolite was also observed on the surface after subjecting a sample to rigorous treatment for 24 h in an ultrasonic bath as described above and shown in Figure 7.

V. Conclusions

Zeolite crystals have been synthesized at metal foil interfaces and characterized by a variety of methods. These

(19) (a) Szostak, R. *Molecular Sieves*; Van Nostrand: New York, 1989; p 191–199. (b) Barrer, R. M. *Hydrothermal Chemistry of Zeolites*; Academic Press: New York, 1982; pp 105–182.
(20) Borgstedt, E. V. R.; Davis, S. P.; Suib, S. L., unpublished results.
(21) Tanguay, J. F.; Suib, S. L. *Catal. Rev. Sci. Eng.* **1987**, *29*, 1–40.
(22) Bartlett, J. R.; Cooney, R. P.; Kydd, R. A. *J. Catal.* **1988**, *114*, 58–70.
(23) Davis, S. P.; Borgstedt, E. V. R.; Fessehaie, M. G.; Willis, W. S.; Suib, S. L., manuscript in preparation.
(24) Creasy, K. E.; Shaw, B. R.; Borgstedt, E. V. R.; Davis, S. P.; Suib, S. L., manuscript in preparation.
(25) (a) Tchernev, D. I. In *Natural Zeolites, Occurence, Properties and Use*; Pergamon Press: New York, 1978; pp 479–485. (b) Gopal, R.; Hollebone, B. R.; Langford, C. H.; Shigeishi, R. A. *Sol. Energy* **1982**, *26*, 178–182. (c) Halacy, D. *Understanding Passive Cooling Systems*; Volunteers in Technical Assistance, Arlington, VA, 1986, TP No. 48, 17.

materials can be prepared with zeolite coatings having thicknesses of tenths of a micron to over a millimeter in thickness depending on the particular synthesis conditions. The films are very stable toward mechanical, chemical, and thermal treatments. A reviewer has suggested that a stirred gel could be used to eliminate gradients during crystallization. This is the focus of current efforts. The chemical composition of the zeolites can be altered by ion-exchange procedures. It is likely that other synthetic procedures like adsorption, sublimation, and incipient wetness can be used to further alter the chemical compositions of these systems. Spectroscopic studies have shown that these zeolites are crystalline and homogeneous. Finally, it appears that there are several exciting possibilities for the use of such materials in the areas of catalysis, electrochemistry,[24] photochemistry, and semiconductor devices.

Acknowledgment. First attempts to make zeolite thin films were initiated in L. R. Faulkner's lab, and we thank him for inspiration and ideas in this area. Helpful discussions with Lennox E. Iton of Argonne National Labs and Professor John Tanaka of the University of Connecticut are gratefully acknowledge. We thank Professor Leo Herbette of the University of Connecticut Health Center for making the synchrotron XRD measurements and Elsie Matthews of Biopolymers, Inc. for conducting the 180° peel strength measurements. Support for this research was from the University of Connecticut Research Foundation and the State of Connecticut Department of Higher Education through the High Technology Grant award program.

Hydrothermal Synthesis and Single-Crystal Structural Characterization of $V_2O_4(C_6H_5AsO_3H)\cdot H_2O$

Guohe Huan,* Jack W. Johnson,* and Allan J. Jacobson

Corporate Research Laboratories, Exxon Research & Engineering Company, Annandale, New Jersey 08801

Joseph S. Merola

Department of Chemistry, Virginia Polytechnic and State University, Blacksburg, Virginia 24061

Received June 12, 1990

The layered compound $V_2O_4(C_6H_5AsO_3H)\cdot H_2O$ has been prepared by hydrothermal synthesis and characterized by single-crystal X-ray diffraction. The structure is monoclinic, space group $P2_1/c$ (No. 14) with a = 12.074 (4) Å, b = 9.574 (3) Å, c = 9.872 (2) Å, β = 107.63 (2)°, and Z = 4 and is formed of undulating layers of vanadium, oxygen, and arsenic atoms with phenyl groups directed into the interlayer space. The phenyl groups from adjacent layers interpenetrate to form a monolayer of organic groups between the inorganic sheets, resulting in a layer repeat distance (d_{100}) of 11.507 (4) Å. The layers contain edge-shared pairs of $V^{5+}O_5$ square pyramids connected through corners to $V^{4+}O_6$ octahedra. The phenylarsonate moiety includes a terminal hydroxyl group that is hydrogen bonded to an oxygen atom of the vanadium oxide framework. The magnetic susceptibility displayed by the new compound follows the Curie–Weiss law in the temperature range 50–350 K, with reduced susceptibility due to antiferromagnetic coupling at temperatures below 50 K.

Introduction

Divalent metal phenylphosphonates and phenylarsonates $MC_6H_5RO_3\cdot xH_2O$ (M = divalent metal, R = P or As, and x = 0, 0.5, and 1) have been known for more than a decade.[1,2] Although no single crystals suitable for structure determination were available, the morphology, color, powder X-ray diffraction patterns, and bulk magnetic properties indicated that these compounds belonged to an isomorphous series with structures in which layers consisting of octahedrally coordinated metal ions linked by multibridging acid groups are held together by weak van der Waals forces.[2] The structure of $MnC_6H_5PO_3\cdot H_2O$ was reported recently.[3] It consists of roughly coplanar layers of manganese atoms coordinated by phenylphosphonate groups arranged above and below the plane of the manganese atoms and can be described as $MnO_{1/2}O_{4/3}(H_2O)_{1/1}C_6H_5PO_{1/2}O_{2/3}$. Each Mn atom is octahedrally coordinated by five phosphonate oxygen atoms and one water molecule. $ZnC_6H_5PO_3\cdot H_2O$ is essentially isostructural[4] with the Mn analogue. Microcrystalline $VOC_6H_5PO_3\cdot 2H_2O$ was prepared in this laboratory[5] by refluxing phenylphosphonic acid with V_2O_5 in 95% ethanol/water. The proposed structure can be described as $VO_{1/1}O_{3/2}(H_2O)_{2/1}C_6H_5PO_{3/2}$ and is analogous to that of the mineral newberyite,[6] $MgHPO_4\cdot 3H_2O$. Very recently, we have prepared single crystals of $VOC_6H_5PO_3\cdot H_2O$ by

(1) Sandhu, S. S.; Sandhu, G. K. *J. Inorg. Nucl. Chem.* **1972**, *34*, 2249–2253.
(2) Cunningham, D.; Hennelly, P. J. D.; Deeney, T. *Inorg. Chim. Acta* **1979**, *37*, 95–102.
(3) Cao, G.; Lee, H.; Lynch, V. M.; Mallouk, T. E. *Inorg. Chem.* **1988**, *27*, 2781–2785.
(4) Martin, K.; Squattrito, P. J.; Clearfield, A. *Inorg. Chim. Acta* **1989**, *155*, 7–9.
(5) Johnson, J. W.; Jacobson, A. J.; Brody, J. F.; Lewandowski, J. T. *Inorg. Chem.* **1984**, *23*, 3842–3843.
(6) Sutor, D. J. *Acta Crystallogr.* **1967**, *23*, 418–422. Abbona, F.; Boistelle, R.; Haser, R. *Acta Crystallogr.* **1979**, *B35*, 2514–2518.

0897-4756/90/2802-0719$02.50/0